

TITLE:Influence of Seed Layer Moduli on FEM Based Modulus Backcalculation Results

Kunihito MATSUI

Professor

Dept. of Civil and Environmental Engineering, Tokyo Denki University

Hatoyama-Cho, Hiki-Gun, Saitama 350-0394, Japan

Tel.: +81-492-96-2911

Fax: +81-492-96-6501

matsui@g.dendai.ac.jp

Yoshitaka HACHIYA

Head

Airport Facilities Division, National Institute for Land and Infrastructure Management, Ministry of Land,
Infrastructure and Transport

1-1, Nagase 3, Yokosuka, 239-0826, Japan

Tel: +81-468-44-5034

Fax: +81-468-44-4471

hachiya@ipc.ysk.nilim.go.jp

James W. MAINA

CSIR, P O Box 395,

Pretoria, 0001, South Africa

Tel.: +27-12-841-3956

Fax: +27-12-841-3232

JMaina@csir.co.za

Yukio KIKUTA

Professor

Dept. of Civil and Environmental Engineering, Kokushikan University

4-28-1 Setagaya, Setagaya-Ku, Tokyo 154-8515, Japan

Tel.: +81-3-5481-3279

Fax: +81-3-5481-3279

kikuta@kokushikan.ac.jp

Tasuku NAGAE

Graduate student

Dept. of Civil and Environmental Engineering, Tokyo Denki University

Hatoyama-Cho, Hiki-Gun, Saitama 350-0394, Japan

Tel.: +81-492-96-2911

Fax: +81-492-96-6501

TOTAL NUMBER OF WORDS (including abstract, figures and tables):7,370

ABSTRACT

Determination of pavement layer moduli from FWD test data is known as backcalculation analysis. Generally, backcalculation analysis is an unstable procedure which is greatly influenced by several types of error causes. These errors may be categorized as modeling error in the forward analysis, deflection measurement error, numerical computation error due to instability in the backcalculation procedure, etc. Because of all the problems mentioned, selection of seed values for layer moduli would highly influence backcalculation results.

In order to reduce effects of measurement error, truncated singular value decomposition is utilized in backcalculation for regularization purpose. Scaling of variables, which is often used in optimization algorithm, is implemented to improve numerical accuracy. In dynamic backcalculation, Ritz vector reduction method is employed to efficiently solve a large system of dynamic equations. Various other means are also introduced to cut down computation time.

This paper presents recent updates of DBALM (Dynamic Back Analysis for Layer Moduli) software whose solver is based on axi-symmetric FEM and was first developed in 1993. Examples on airfield pavement application are also presented. The results are compared with results from our static backcalculation software BALM (Back Analysis for Layer Moduli) where the solver was developed using multilayered linear elastic theory. From our experience, we believe a dynamic backcalculation is superior to static backcalculation. The difference between the results from the two methods is presented in this paper.

INTRODUCTION

Falling weight deflectometer (FWD) is widely used as a standard nondestructive testing device for structural evaluation of pavements. Several highway and airport agencies have, in recent years, been drawing up their pavement maintenance and management plans based on FWD test results. A wrong interpretation of the FWD test results may lead to very high maintenance and management costs. FWD is a dynamic test, which applies impulsive force to the pavement surface. However, conventional approach to estimate layer moduli is so called static backcalculation, where peak load and corresponding peak deflections are considered as the responses of a quasi-static deflection called deflection bowl. Intensive comparison of static backcalculation software may be found in, for example, (1).

It is well known that the differential equation of motion can be written as,

$$m \frac{d^2 z}{dt^2} + c \frac{dz}{dt} + kz = F_0 \sin \omega t \quad (1)$$

where ω is the frequency of the harmonic excitation. The steady state solution of the above equation becomes,

$$\frac{Z}{Z_0} = \frac{1}{\sqrt{[1 - (\omega/\omega_n)^2]^2 + [2\zeta(\omega/\omega_n)]^2}} \quad (2)$$

where:

$$\omega_n = \sqrt{k/m} = \text{natural frequency of undamped oscillation in radian per second,}$$

$$\zeta = c/c_0 = \text{damping factor, and}$$

$$Z_0 = F_0/k = \text{zero frequency deflection of the spring-mass system under the action of steady}$$

force F_0 .

Eq.(2) is called a magnification factor and is graphically represented as shown in Figure 1. The figure shows that the response of one degree of freedom system does not in general coincide with static deflection. Thus, if we apply static backcalculation to dynamic data, we may obtain false results.

FWD is a dynamic test. Generally, depending on the type of the FWD device, a one or two mass force generating unit is dropped on un-segmented plate with thin hard rubber pad or segmented plate with thick, soft rubber pad, which is placed on the pavement surface. The impact force generates radially propagating shockwaves. Waves (deflection forms), in the vertical direction, caused by the impact load are measured at several points on concentric circles with different radii whose centers are located at the center of the loading plate. Duration of loading runs from 20 ms to 65 ms depending on the type of FWD device. FWD provides rich information if it is fully utilized. Considering peak values for each measurement points, it becomes clear that points farther from the center of loading attain their peak values later than points closer to the center of loading. This time difference is known as phase difference of deflections and is considered the velocity of propagation of the shockwaves. Furthermore, it is also well known that velocity of wave propagation in pavement structures will be different depending on frequency of the shockwaves. These types of time series data contain useful information that if well utilized would contribute to improved accuracy in structural pavement evaluation. The use of only peak values implies discarding the rich information. It is essential from now on to find out how to make use of FWD time series data and what kind of information we can extract from it.

Static backcalculation can identify pavement layer moduli from the peak loading and the corresponding peak deflections. It is known that, under the same peak loading, the longer the loading duration the larger the surface deflection becomes (2). That is why static backcalculation tends to yield larger stiffness. Several authors have presented dynamic backcalculation of FWD time series data (3-6). They have not stated in detail, methods of backcalculation and the algorithms used. In the past, some of authors of this paper proposed a method for dynamic backcalculation of pavement layer moduli using time series FWD data (2, 7-11).

Backcalculation analysis is known to be intrinsically unstable. Its success depends on the selection of algorithm coupled with regularization technique implemented in the algorithm (7). Authors use the Gauss-Newton method with truncated singular value decomposition with scaling of variables. Scaling of variables is recommended for solving optimization problems when parameter values are different in order (12). It seems the scaling is particularly useful for dynamic backcalculation since damping coefficients are much smaller than layer moduli. In static backcalculation, which is called BALM (Static Analysis for Layer Moduli), elastic multilayered analysis software called GAMES (13), is used to compute pavement responses. However, because FEM is employed to compute pavement responses in our dynamic backcalculation (DBALM), equations of motion result in a large system of differential equations. If we solve the system of equations, computational time becomes enormous and dynamic backcalculation impractical. A matrix reduction method based on Ritz vectors (14) is introduced in the analysis of dynamic system and more than 500 equations of motion are reduced to 30 equations, which yields a drastic reduction of computational time.

Average surface deflections of three or four sets of test data are conventionally used in static backcalculation in order to reduce effects of measurement error. However, averaging of time series data for the backcalculation use is questionable. We have developed backcalculation algorithm, which can handle multiple sets of data simultaneously with little increase of computation time (10). Although the dynamic backcalculation is still time consuming as compared with the static backcalculation, it conforms well to the characteristics of FWD test and the results obtained seem to be more reliable than the results from static method.

The objectives of this research are, 1) to evaluate influence of seed moduli on backcalculation results, 2) to apply the DBALM to the airfield data taken at test site, 3) to compare results from static and dynamic backcalculation analyses and 4) to estimate layer damping coefficients.

EQUATIONS OF MOTION AND SENSITIVITY ANALYSIS

Since FWD test applies an impulsive load on the surface of a pavement structure, dynamic and not static backcalculation should ideally be used to determine pavement layer moduli as well as damping coefficients. Dynamic forward analysis is required in order to perform dynamic backcalculation. Equation of motion for the impulsive FWD loading can be presented as follows:

$$\left. \begin{aligned} \mathbf{M} \frac{d^2 \mathbf{z}^{(l)}}{dt^2} + \mathbf{C} \frac{d\mathbf{z}^{(l)}}{dt} + \mathbf{K} \mathbf{z}^{(l)} &= \mathbf{f} g^{(l)}(t) \\ \mathbf{z}^{(l)}(0) &= \mathbf{0}, \quad \frac{d\mathbf{z}^{(l)}}{dt}(0) = \mathbf{0} \end{aligned} \right\} \quad (3)$$

where; \mathbf{M} , \mathbf{C} , \mathbf{K} represent mass, damping and stiffness matrices, respectively. \mathbf{K} is a function of layer moduli, $\mathbf{E} = \{E_j\}$, ($j = 1, 2, \dots, M$), and \mathbf{C} is a function of layer damping coefficients, $\mathbf{Q} = \{Q_j\}$, ($j = 1, 2, \dots, M$). M is a total number of pavement layers, \mathbf{f} is nodal load distribution vectors, $g^{(l)}(t)$ is a scalar representation of load as a function of time for the l^{th} time series loading measurement. \mathbf{f} can be formulated considering uniform distribution of load over a loading plate of radius a . Eight nodes iso-parametric elements are utilized in the finite element analysis. By assembling element stiffness matrices, a layer stiffness matrix can be obtained. The stiffness matrix \mathbf{K}_j for the j^{th} layer is a function of E_j and can be written as $E_j \mathbf{H}_j$, ($j = 1, 2, \dots, M$). Similarly, damping matrix \mathbf{C}_j , which is a function of Q_j can be written as $Q_j \mathbf{H}_j$. This implies that E_j in stiffness matrices of all elements in every pavement layer can be replaced by Q_j to obtain damping matrices. \mathbf{H}_j is composed of only nodal coordinates in j^{th} layer. \mathbf{M} , \mathbf{H}_j as well as \mathbf{f} can be prepared during the first iteration step and remain unchanged in subsequent iterations. A global stiffness matrix, \mathbf{K} is constructed from layer stiffness matrix, $\mathbf{K}_j = E_j \mathbf{H}_j$ while a global damping matrix, \mathbf{C} is from $\mathbf{C}_j = Q_j \mathbf{H}_j$. Since every term in Eq. 1 has a unit of force and the unit of E_j is Pa or N/m^2 , the unit of Q_j will be $\text{N} \cdot \text{s}/\text{m}^2$.

It is important to perform sensitivity analysis of deflections with respect to the unknown parameters during backcalculation analysis. Derivatives of deflections with respect to E_j and Q_j in Eq. 1 can be written as follows:

$$\mathbf{M} \frac{d^2}{dt^2} \left(\frac{\partial \mathbf{z}^{(l)}}{\partial E_j} \right) + \mathbf{C} \frac{d}{dt} \left(\frac{\partial \mathbf{z}^{(l)}}{\partial E_j} \right) + \mathbf{K} \frac{\partial \mathbf{z}^{(l)}}{\partial E_j} = - \frac{\partial \mathbf{K}}{\partial E_j} \mathbf{z}^{(l)} \quad (4)$$

$$\mathbf{M} \frac{d^2}{dt^2} \left(\frac{\partial \mathbf{z}^{(l)}}{\partial Q_j} \right) + \mathbf{C} \frac{d}{dt} \left(\frac{\partial \mathbf{z}^{(l)}}{\partial Q_j} \right) + \mathbf{K} \frac{\partial \mathbf{z}^{(l)}}{\partial Q_j} = - \frac{\partial \mathbf{C}}{\partial Q_j} \frac{d \mathbf{z}^{(l)}}{dt} \quad (5)$$

Since the differential operators in Eqs. 4 and 5 are similar to Eq. 3, the same method is used to solve for $\partial z_i^{(l)} / \partial E_j$ and $\partial z_i^{(l)} / \partial Q_j$.

The sizes of Eqs. 3, 4 and 5 are reduced by using Ritz vectors (12). The reduced system of equations is rewritten as a first order system of differential equations, which is solved analytically by using an eigenvalue analysis (8).

SCALING OF VARIABLES AND BACKCALCULATION ANALYSIS

The process of determining pavement layer moduli and damping coefficients using measured data is referred to as backcalculation analysis. These parameters are determined such that there is a good match between computed and measured deflections. It is imperative that measurements of time series loading and deflection data be made simultaneously. Contrary to static backcalculation, synchronization of the data is essential in dynamic backcalculation. In order to match both computed and measured deflections, an evaluation function is defined as:

$$J = \frac{1}{2LN} \sum_{l=1}^L \int_{t_0}^{t_1} \sum_{i=1}^N \left\{ u_i^{(l)}(t) - z_i^{(l)}(\mathbf{X}, t) \right\}^2 dt \quad (6)$$

where J is the least square function and $\mathbf{X} = (X_1, X_2, \dots, X_{2M})^T$ is a vector of the scaled unknown parameters.

$u_i^{(l)}(t)$ is the l^{th} time series deflection at sensor point i , while $z_i^{(l)}(\mathbf{X}, t)$ is analytical deflection at sensor point i due to l^{th} time series load measurement. L is number of data sets and N is number of sensors. The scaling of variables is considered important when the order of variables is different (12).

Iterative computation is necessary because determination of \mathbf{X} is a nonlinear minimization problem. Taylor expansion may be used as follows:

$$z_i^{(l)}(\mathbf{X} + d\mathbf{X}, t) = z_i^{(l)}(\mathbf{X}, t) + \sum_{j=1}^{2M} \frac{\partial z_i^{(l)}}{\partial X_j} dX_j \quad (7)$$

Substituting Eq. 7 into Eq. 6, and simplify to obtain Eq. 8 as:

$$\mathbf{A} \Delta \mathbf{X} = \mathbf{b} \quad (8a)$$

where

$$\mathbf{A} = \left[\sum_{j=1}^{2M} \int_0^{t1} \sum_{\lambda=1}^L \left(\sum_{i=1}^N \frac{\partial z_i^{(l)}}{\partial X_j} \frac{\partial z_i^{(l)}}{\partial X_k} \right) dt \right] \quad (8b)$$

$$\Delta \mathbf{X} = \{ \Delta X_j \} \quad (j = 1, 2, \dots, 2M) \quad (8c)$$

$$\mathbf{b} = \int_0^{t1} \sum_{\lambda=1}^L \sum_{i=1}^N \left\{ \left(u_i^{(l)}(t) - z_i^{(l)}(\mathbf{X}, t) \right) \frac{\partial z_i^{(l)}}{\partial X_k} \right\} dt \quad (k = 1, 2, \dots, 2M) \quad (8d)$$

\mathbf{A} is $M \times M$ square matrix, $\Delta \mathbf{X}$ and \mathbf{b} are $2M \times 1$ vectors. Eq. 8a represents simultaneous linear equations, which should be solved with care because there may be some instances when the determinant of \mathbf{A} tends to zero. $\partial z_i^{(l)} / \partial X_j$ is a function of time and can be determined from Eq. 9 as:

$$\frac{\partial z_i^{(l)}}{\partial X_j} = E_j^0 \frac{\partial z_i^{(l)}}{\partial E_j} \quad (j = 1, \dots, M) \quad (9a)$$

$$\frac{\partial z_i^{(l)}}{\partial X_{j+M}} = Q_j^0 \frac{\partial z_i^{(l)}}{\partial Q_j} \quad (9b)$$

where E_j^0 and Q_j^0 are seed modulus and damping coefficient of j^{th} layer. $\partial z_i^{(l)} / \partial E_j$ and $\partial z_i^{(l)} / \partial Q_j$ can be obtained by solving Eqs. 4 and 5.

Considering unstable nature of this set of equations, singular value decomposition is used. \mathbf{A} is decomposed as,

$$\mathbf{A} = \mathbf{U} \mathbf{D} \mathbf{V}^T \quad (10)$$

in which $\mathbf{U}^T \mathbf{U} = \mathbf{V} \mathbf{V}^T = \mathbf{1}$ is a unit matrix and \mathbf{D} is a diagonal matrix composed of singular values. The value of maximum singular value divided by minimum singular value is called condition number. By using these decomposed matrices, the solution of linear set of equations can be written as,

$$\Delta \mathbf{X} = \mathbf{V} \mathbf{D}^{-1} \mathbf{U}^T \mathbf{b} \quad (11)$$

The above equation can be rewritten as,

$$\Delta \mathbf{X} = \sum_{i=1}^M a_i \mathbf{v}_i \quad (12)$$

where \mathbf{v}_i is i^{th} column of \mathbf{V} and $a_i = \frac{1}{d_{ii}} \sum_{j=1}^M U_{ji} b_j$. U_{ji} is the (i, j) element of \mathbf{U} , b_j is the j^{th}

element of \mathbf{b} and d_{ii} is (i, i) element of \mathbf{D} . If d_{ii} is smaller than a threshold value, a_i is computed such that $1/d_{ii}$ is taken as 0 to prevent a significant influence of measurement error involved in b_j . The threshold value is chosen as 0.001 of maximum singular value in our software.

Assuming initial values for unknown parameters and updating the parameters after each iterative step, the computations must be repeated until a convergence is achieved. However a convergence will never be achieved unless some regularization technique is introduced. A truncated singular value decomposition, which is the simplest and the most efficient one among regularization techniques if a proper threshold value is selected, is implemented in DBALM.

ACCELERATED PAVEMENT TEST (APT) DATA (13)

Two experimental pavements, Section A and Section B, were constructed in a reinforced concrete vessel as shown in Figure 2. After construction, the aircraft load simulator, which can simulate the wheel loading of B747-400 aircraft (910 kN), was used to apply 10,000 load repetitions in a bi-directional mode at a speed of 5 km/h. The position of the wheel path was as shown in Figure 2. After 5,000 load repetitions, it was impossible to continue the test due to excessive rutting for the operation of the aircraft load simulator. The surfaces of both sections were, thereafter, repaired using the same materials as that of the surface course in section A before continuing with the remaining 5,000 load repetitions. In this paper, data for the first 5,000 load repetitions at Section B is used.

After every specified number of load repetitions, FWD tests were performed along the wheel path as shown in Figure 2. The diameter of the FWD loading plate was 450 mm and a loading level of 250 kN were used to obtain deflections at 0, 300, 450, 600, 900, 1,500, 2,500 mm from the center of the loading plate. One measurement consisted of four FWD tests and time series loading and deflection data were recorded at an interval of 0.0002 second. Thermocouples embedded in the surface and binder courses were used to measure internal temperatures in the asphalt concrete during the FWD tests.

BACKCALCULATION OF APT DATA

Time series loading and deflection data measured by FWD were used in a dynamic backcalculation program DBALM, while by using the peak values of loads and deflections, static backcalculation was conducted using BALM software.

Influence of seed layer moduli

Investigation on the influence of seed layer moduli was carried out by performing static and dynamic backcalculation analyses using 1000 sets of seed layer moduli, (ranges: $1,000\text{MPa} < E_1 < 10,000\text{MPa}$, $100\text{MPa} < E_2 < 500\text{MPa}$ and $50\text{MPa} < E_3 < 150\text{MPa}$) which were prepared using uniform random numbers in order to investigate seed value effects. Backcalculation was performed statically and dynamically. FWD tests were conducted four times under the same condition. After modifying the measured deflections to the standard 250 kN, surface deflections were averaged and used to perform static backcalculation using the averaged values. However for dynamic backcalculation, new algorithm was developed which has similar to the effect of averaging static deflections (10). Figure 4a shows the meshing of pavement section and Figure 4b is a set of measured load and surface deflections data. Time increment used for the dynamic analysis is 0.002 second to reduce computational time, although measurement is taken at every 0.0002 second. When performing dynamic backcalculation, the measured surface deflections between t_0 and t_1 are matched with computed deflections of the same range, while applied load data of the range between 0 and t_1 is used for dynamic analysis.

Both static and dynamic backcalculation results before the application of wheel load are plotted in Figure 4. It is observed that static results vary in relatively small range compared with dynamic results. The mean values of results are $E_1 = 14410\text{ MPa}$, $E_2 = 330\text{ MPa}$, $E_3 = 80\text{ MPa}$ for static backcalculation and $E_1 = 9380\text{ MPa}$, $E_2 = 150\text{ MPa}$, $E_3 = 70\text{ MPa}$ for dynamic backcalculation. Temperature at the middle of asphalt concrete is 9.7°C . Since layer damping coefficients can be estimated from dynamic backcalculation, they are also described in Figure 4. Static backcalculation results are larger than dynamic backcalculation results. This is a general trend which has been observed in the past. Since the values of base modulus scatters widely, two sets of initial values corresponding to the largest and smallest of base moduli in Figure 4(b) are selected, the iteration processes for static and dynamic backcalculations are plotted in Figure 5. The figure demonstrates steady convergence. Possible cause of larger scatter for dynamic backcalculation is difference in the number of unknown parameters, three for static backcalculation and six for dynamic backcalculation.

Figure 6 shows comparison of measured and computed deflections after convergence is achieved. Good match of deflections is observed. However, a slight phase difference is observed because the time corresponding to peak measured deflections appear to be different from the time corresponding to peak computed deflections. Records of loading and deflections must be well synchronized when dynamic backcalculation is performed.

Figure 7(a) shows a sample of measured load and deflections where peak points are marked. Figure 7(b) illustrates a deflection bowl formed from peak surface deflections in Figure 7(a) and surface deflection obtained from static analysis by using layer moduli from dynamic backcalculation and peak load. It is obvious that the deflection bowl is much smaller than the static deflection. Thus, if the deflection bowl is considered as static deflection, backcalculated moduli are expected to be larger. This is the reason why static backcalculation results become greater than dynamic results.

During the accelerated pavement loading test, FWD tests were performed at 0, 50, 100, 200, 500, 1000, 2000, 3000, 5000 load repetitions. Maximum, mean and minimum backcalculation results are illustrated in Figure 8. As number of repeated loading increases, layer moduli decreases. It is observed that scatter in static backcalculation results is much smaller than dynamic one. The scatter for static case decreases with increasing number of loading, while that for dynamic backcalculation remains nearly same.

APPLICATION TO OTHER FWD DATA

LTPP data at Site 3, State highway 281, Texas (16)

More evaluations, with the objective of confirming the accuracy and suitability of the software used for dynamic analysis in this research, were performed also using data obtained from the webpage under TRB committee A2B05. Among the data released to the public through Nonlinear Pavement Analysis Project under the Committee, only data from Site 3, which is located on State Highway 281, Texas were used.

The pavement structure on this section was as follows: 203mm surface layer (asphalt concrete), 308 mm flexible base (no treatment) and the subgrade soil, which was clayey and moderately stress-dependent. In this site, bedrock was located at a depth of 1.9 m below the pavement surface. Four types of loading (27, 40, 53, 71 kN) were applied during FWD testing, with 3 drops per each load. Furthermore, 6 deflection sensors located at 0, 305, 610, 915, 1220, 1525 mm from the center of the loading plate were used to record vertical deflections. Seed moduli used here are same as those of the aircraft load simulator data in the previous section. Backcalculation results presented here are those corresponding to 71kN. The FWD load plate was positioned at approximately 220mm from the multi-depth deflectometer (MDD) cap. The MDD recorded the pavement's deflections at three different depths, which were approximately 95 mm (AC layer), 314mm (base course layer) and 594 mm (subgrade layer) from the surface of the pavement. Figure 9 shows the results from static and dynamic backcalculation. Figure 10 presents the comparison of measured and computed surface deflections and the comparison of measured and computed vertical displacements at MDD sensor locations. The vertical displacements at MDD sensor locations are computed by DynaPave3 (II) which is dynamic analysis solver for pavement implemented in DBALM.

Road Test Sections in Japan

Figure 11 shows 2 types of pavement sections where FWD tests were conducted. The two sections were constructed side by side with similar base and subgrade materials. Thickness of asphalt concrete layer for section C was 5.1 cm while that of section D was 24.6 cm. Past experience with backcalculation analysis has shown that different seed moduli almost always give different backcalculation results and this trend is very prominent in case the thickness of surface course is less than 7.5 cm. It is with this respect that experience is very important for good selection of seed moduli in backcalculation analysis. In this research, random numbers were used to generate seed values for layer moduli and the influence thereof was investigated.

By using the 1000 sets of seed values, E_1 between 1,000 MPa and 10,000MPa, E_2 between 100 MPa and 500 MPa, E_3 between 80 MPa and 300 MPa, and E_4 between 50 MPa and 150 MPa, static and dynamic backcalculation were conducted and the results are described in Figures 12 and 13 respectively. Figure 12(a) and (b) are static backcalculation results for section C and section D. Although both sections are composed of similar materials, asphalt concrete layer modulus of section C ($E_1 = 8,000$ MPa) is greater than that of section D ($E_1 = 5,000$ MPa), while subgrade modulus of section C ($E_4 = 80$ MPa) is smaller than that of section D ($E_4 = 100$ MPa). By comparing layer modulus in Figures 13(a) and 13(b), it is found that the corresponding layers of sections C and D are nearly same. Layer damping coefficients for section C run between $17.8\text{kN}\cdot\text{s/m}$ and $58.9\text{kN}\cdot\text{s/m}$ for C_1 , between $1.82\text{kN}\cdot\text{s/m}$ and $2.04\text{kN}\cdot\text{s/m}$ for C_2 , between $1.22\text{kN}\cdot\text{s/m}$ and $1.66\text{kN}\cdot\text{s/m}$ for C_3 and between $0.217\text{kN}\cdot\text{s/m}$ and $0.247\text{kN}\cdot\text{s/m}$ for C_4 . And the damping coefficients for section D are between $28.2\text{kN}\cdot\text{s/m}$ and $43.2\text{kN}\cdot\text{s/m}$ for C_1 , between $1.25\text{kN}\cdot\text{s/m}$ and $2.61\text{kN}\cdot\text{s/m}$ for C_2 , between $0.832\text{kN}\cdot\text{s/m}$ and $1.922\text{kN}\cdot\text{s/m}$ for C_3 and between $0.158\text{kN}\cdot\text{s/m}$ and $0.351\text{kN}\cdot\text{s/m}$ for C_4 .

CONCLUSIONS

In backcalculation analysis of FWD data, it is common practice to perform static backcalculation even though the FWD test itself is a dynamic test. This research was, therefore, performed based on the “dynamic analysis should be performed on FWD data” point of view. The following conclusions were drawn based on the results obtained:

1. Static backcalculation in general yields estimates of layer moduli larger than dynamic backcalculation does.
2. Dynamic backcalculation tend to yield larger scatter than static backcalculation when asphalt concrete is thicker. The possible reason is that number of unknown parameters for dynamic backcalculation is as twice as that of static backcalculation
3. Because dynamic backcalculation simulate FWD test, dynamic backcalculation analysis were more reliable than results from static method. However further updates of DBALM is necessary to reduce effects of seed values.
4. Backcalculated results, especially for upper layers in a pavement structure, were highly affected by the seed moduli.
5. Results from TRB data indicate that DBALM and DynaPave3 give sufficiently accurate and acceptable results.
6. Layer damping coefficients also can be identified by DBALM.

At this stage, it is assumed that layer damping coefficients relate to distress of pavement as well as moisture contents. However, further examinations must be made to understand what physically they mean.

ACKNOWLEDGMENTS

Authors of this research study would like to acknowledge the supports by Research Institute of Technology, Tokyo Denki University (Project No. Q02M-05) and Program for Promoting Fundamental Transport (Project No. 2000-03). Authors are also very thankful to Professor Waheed Uddin, University of Mississippi for his advise.

REFERECES

1. Deusen, D.V. : Selection of Flexible Backcalculation Software for the Minnesota road research project, Minnesota Department of Transportation, Aug. 1996.
2. Matsui, K., K. Kikuta, T. Nishizawa, and A. Kasahara. Comparative Studies of Backcalculated Results from FWDs with Different Loading Duration, Nondestructive Testing of Pavement and Backcalculation of Moduli, (Editors: Tayabji, S. D. and E.O. Lukanen) Third Volume, pp. 470-483, March 2000.
3. Uzan, J.: Dynamic Linear Backcalculation of Pavement Material Parameters, *Journal of Transportation Engineering*, ASCE ,Vol. 120(1), pp. 109-126, 1994.
4. Kang, Y. V. Multifrequency Back-Calculation of Pavement-Layer Moduli, *Journal of Transportation Engineering*, vol. 124 (1), pp. 73-81, 1998.
5. Al-Khoury, R., Scarpas, A., Kasbergen, C., and Blaauwendraad, J.: Spectral Element Technique for Efficient Parameter Identification of Layered Media, Part II: Inverse Calculation, *International Journal of Solids and Structures*, Vol. 38, pp. 8753-8772, 2001.
6. Chatti, K., S. W. Haider, H.S. Lee, Y. Ji, and H. Salama. Evaluation of Nonlinear and Dynamic Effects on Asphalt Pavement Response under FWD Loading, *International Journal of Pavements*, Vol. 2, No.1-2, pp. 88-99, 2003.
7. Matsui,K., Nishizawa, T., and Kikuta, Y. Time Domain Backcalculation of Pavement, *Proceedings of Nondestructive Evaluation of Bridges and Highways, SPIE The International Society for Optical Engineering*, March 31- April 3, 1998, San Antonio, Texas, USA.
8. Dong, Q.X., Hachiya, Y., Takahashi, O., Tsubokawa, Y., and Matsui, K. An efficient backcalculation algorithm of time domain for large-scale pavement structures using Ritz vectors, *Finite Element in Analysis and Design* 38 (2002), pp. 1131-1150.
9. Matsui, K., Maina, J. W., Dong, Q., and Sasaki, Y. A Fast Dynamic Backcalculation of Layer Moduli using Axi-Symmetric Approach, *IJP 2003 Volume 2 Number 1-2* January – May 2003, pp. 75 – 87.
10. Maina, J. W., Matsui, K. Kikuta, Y., and Inoue, T. Dynamic Backcalculation of Pavement Structure using Multiple Sets of Time Series data, *ASCE Geo Institute Conference on Geotechnical Engineering for Transportation Projects*, USA, 2004.
11. Maina, J. W., S. Higashi, Y. Kikuta, and K. Matsui. Influence of Seed Values on Dynamic Backcalculation Results, *MAIREPAV4*, Belfast, Aug. 18-20, 2005.
12. Arora, J. S. *Introduction to Optimization*, McGraw Hills, 1989.
13. Maina, J. W. and Matsui, K.: Development Software for Elastic Analysis of Pavement Structure Responses to Vertical and Horizontal Surface Loading, In *Transportation Research Record 1896*, TRB, National Research Council, Washington, D.C., 2004, pp. 107-118.
14. Wilson, E. L., Yuan, M. W., and Dicken, J. M. Dynamic analysis by direct superposition of Ritz vectors, *Journal of Earthquake Engineering and Structural Dynamics* 10 (1982), pp. 813-821.
15. Tsubokawa, Y., Hachiya, Y., Maina, J.W., Nishizawa, T., and Matsui, K. Accelerated Tests on Applicability of Large Stone Asphalt Concretes in Surface Course for Airports, *2nd International Symposium for Accelerated Pavements Test*, Minneapolis, Minn. 2004.
16. <http://www.clrp.cornell.edu/A2B05/>

LIST OF FIGURES

- FIGURE 1 Magnification factor for the vibration of a viscously damped system
- FIGURE 2 Experimental pavement for airfields (aircraft load simulator)
- FIGURE 3 Example of mesh and interval of evaluation function (aircraft load simulator)
- FIGURE 4 Comparison of static and dynamic results for airfield pavement (aircraft load simulator)
- FIGURE 5 Iteration process (aircraft load simulator)
- FIGURE 6 Comparison of measured and computed deflections (aircraft load simulator)
- FIGURE 7 Measured FWD data, and comparison of deflection bowl and static deflection (aircraft load simulator)
- FIGURE 8 Maximum, mean and minimum modulus with respect to loading repetitions (aircraft load simulator)
- FIGURE 9 Frequency distributions of static and dynamic backcalculation results (Texas LTPP data)
- FIGURE 10 Surface deflections and vertical displacements at MDD sensor locations (Texas LTPP data)
- FIGURE 11 Road test sections in Japan
- FIGURE 12 Frequency distributions of static backcalculation (test site in Japan)
- FIGURE 13 Frequency distributions of dynamic backcalculation (test site in Japan)

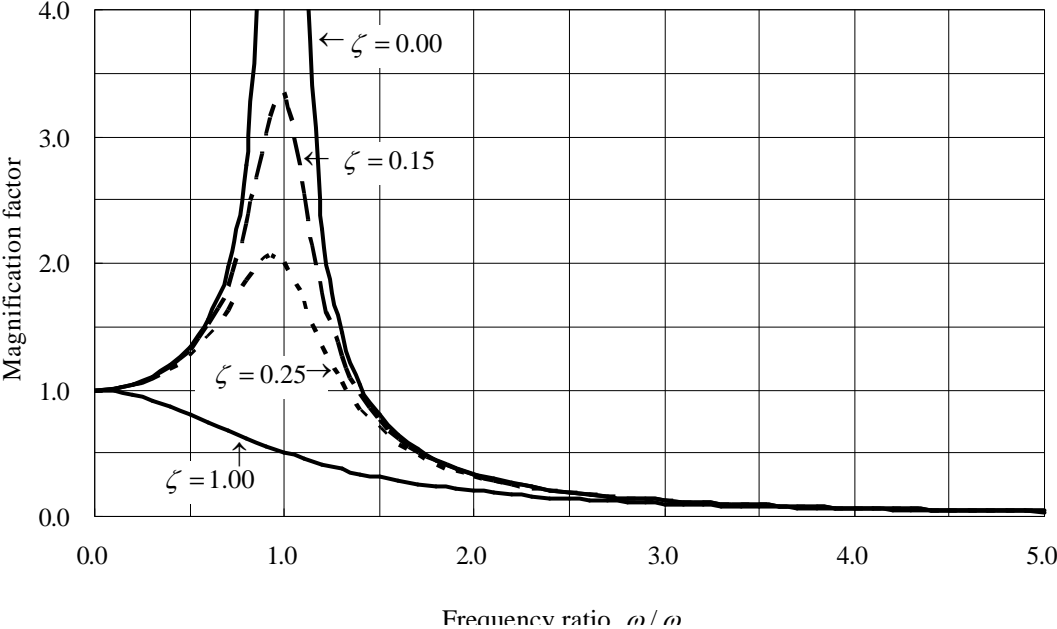
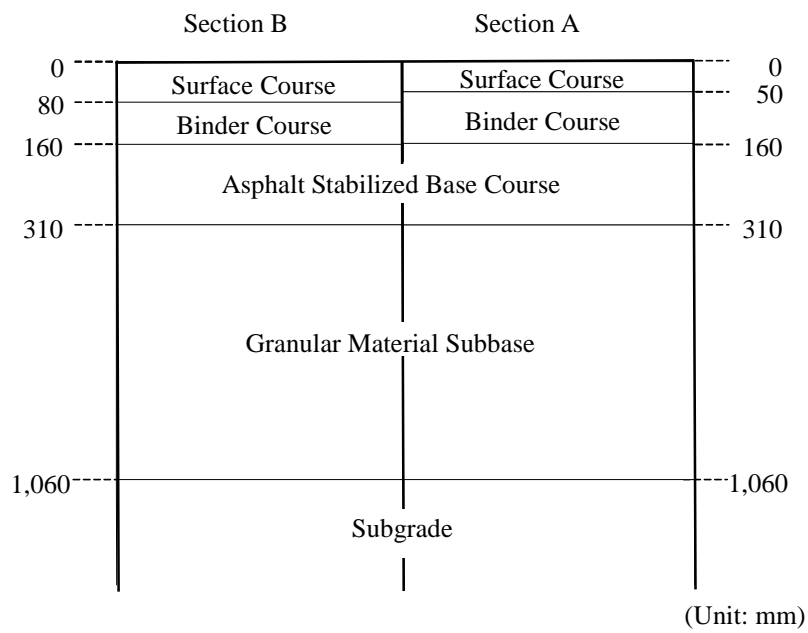
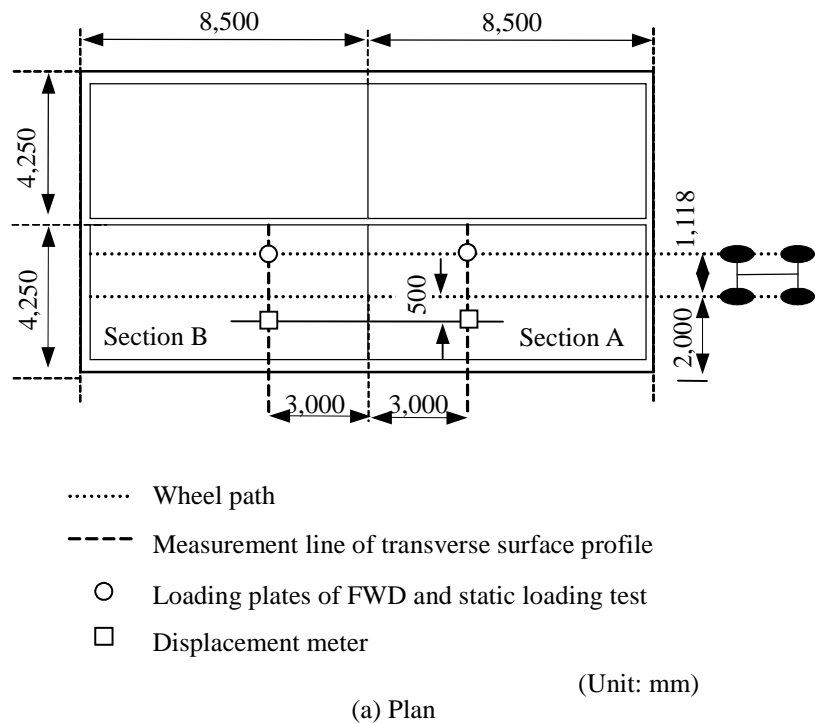
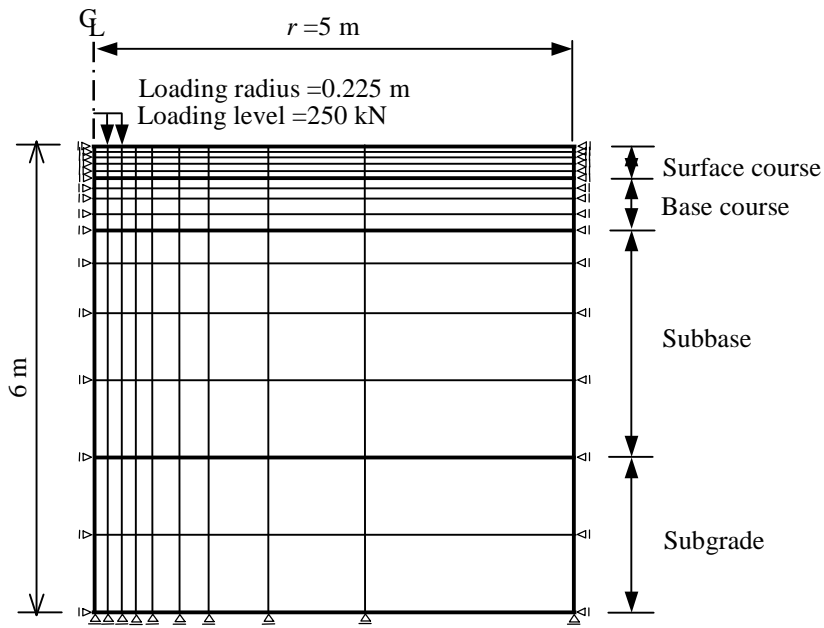


FIGURE 1 Magnification factor for the vibration of a viscously damped system.

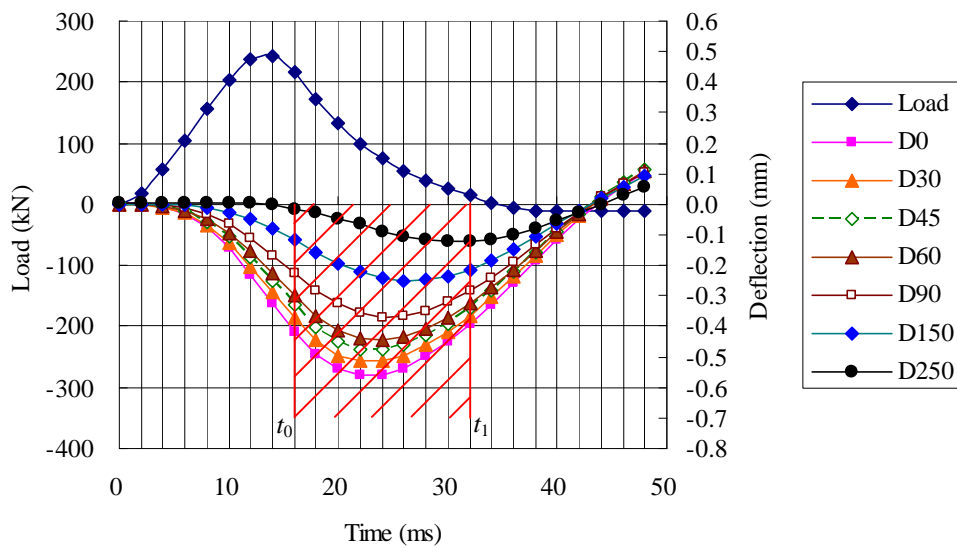


(b) Pavement Section

FIGURE 2 Experimental pavement for airfields (aircraft load simulator).

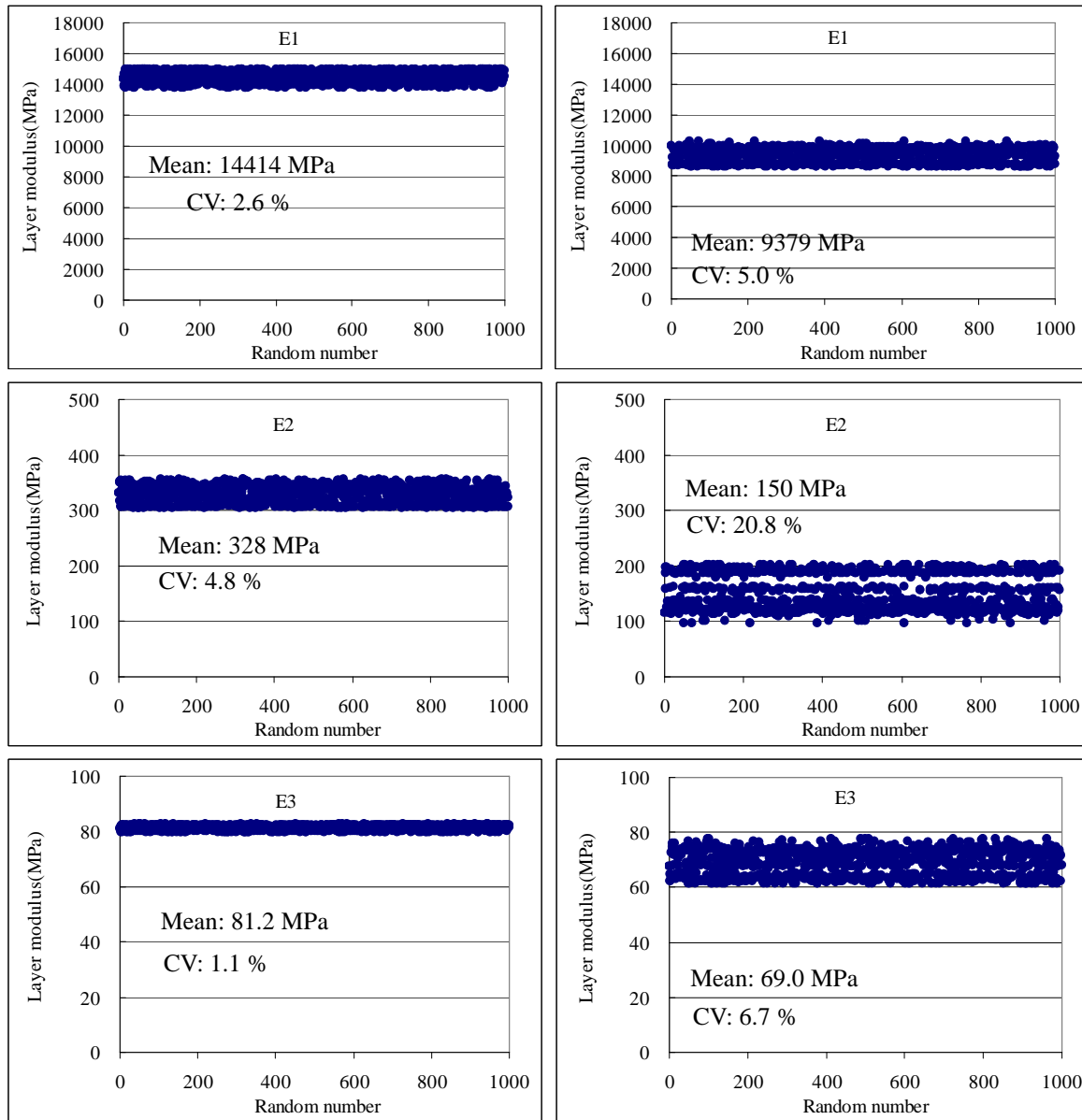


(a) Mesh



(b) Interval of evaluation function (t_0-t_1)

FIGURE 3 Example of mesh and interval of evaluation function (aircraft load simulator).



(a) Static

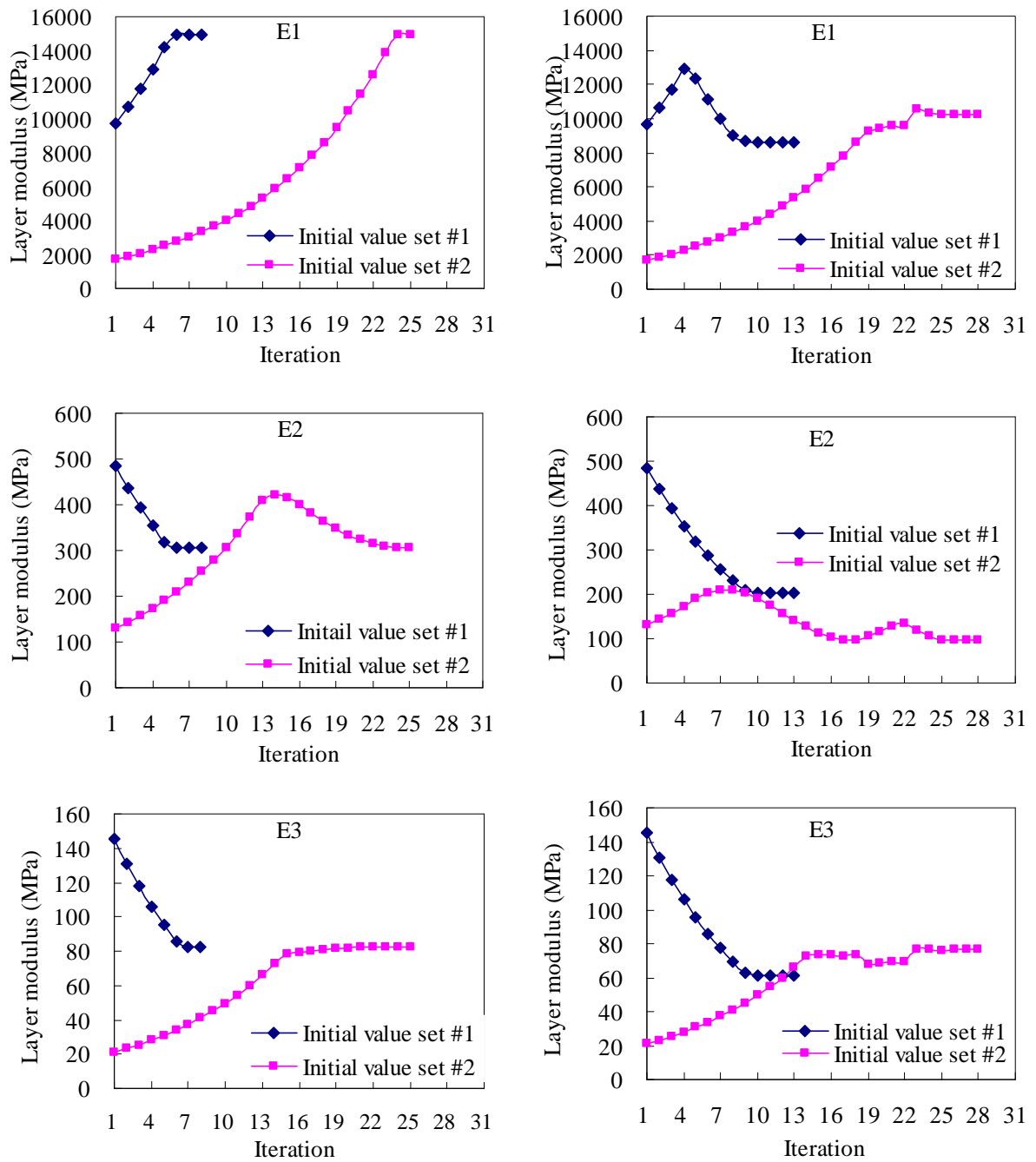
(b) Dynamic

Layer damping coefficients

	C1	C2	C3
Max (kN□s/m)	65.6	2.98	0.325
Min (kN□s/m)	32.9	1.99	0.179
Mean (kN□s/m)	50.7	2.59	0.253
CV (%)	15.0	9.4	13.0

FIGURE 4 Comparison of static and dynamic results for airfield pavement (aircraft load simulator).

(CV : Coefficient of Variation)



(a) Static backcalculation

(b) Dynamic backcalculation

FIGURE 5 Iteration process (aircraft load simulator).

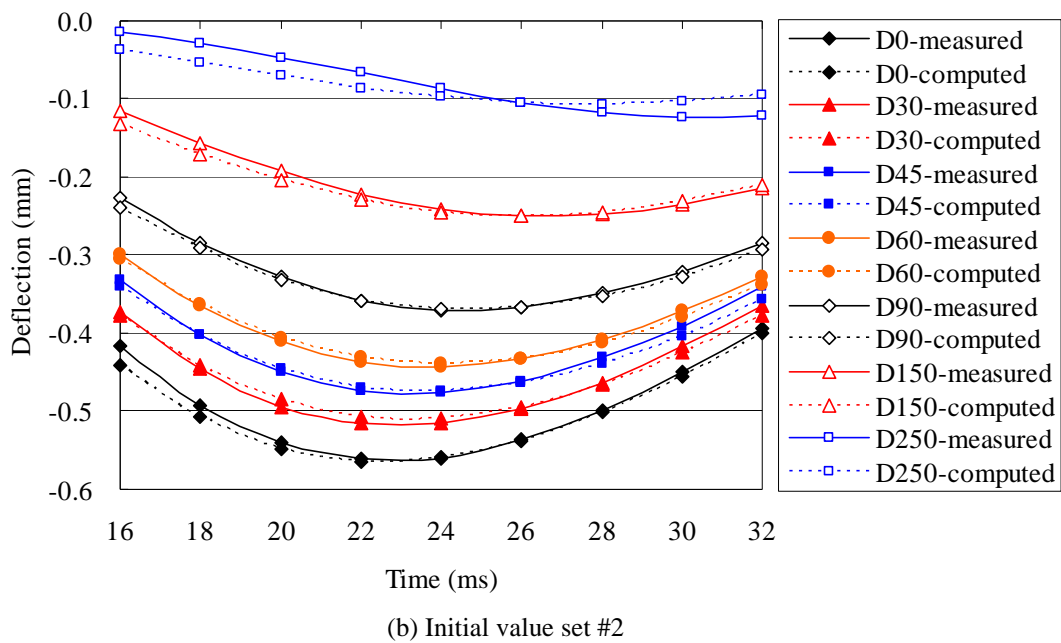
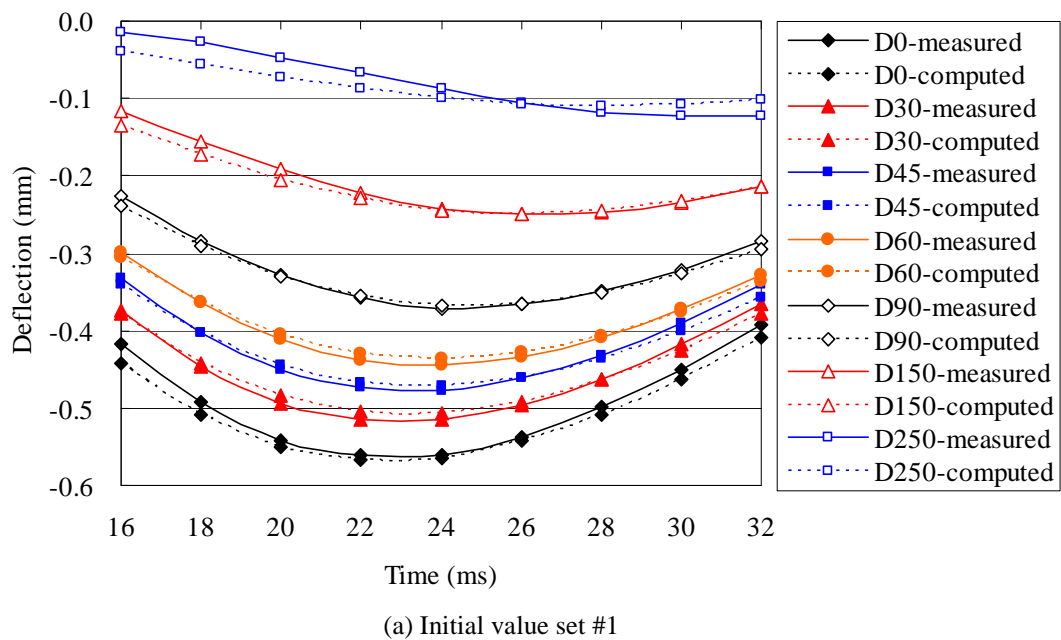
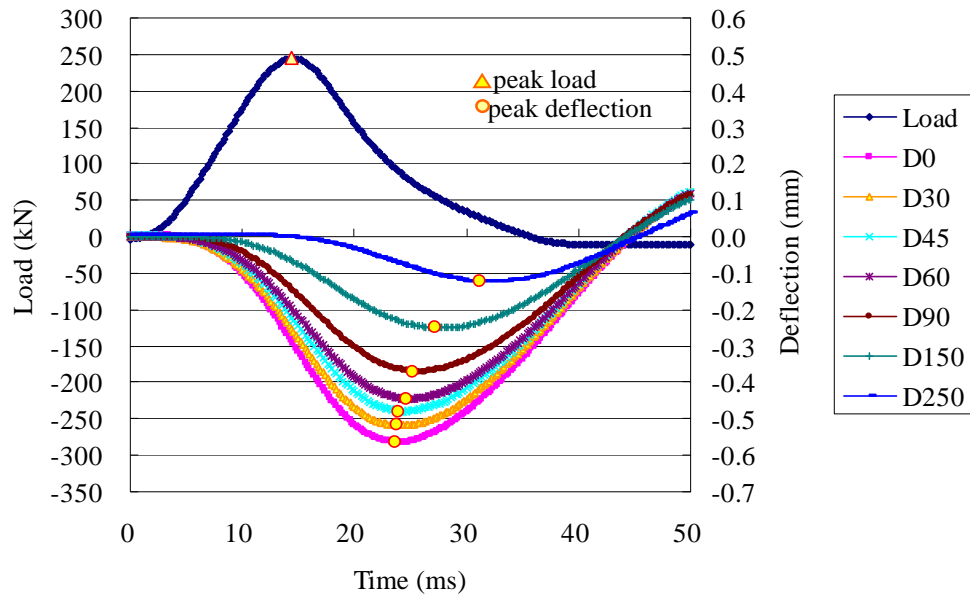
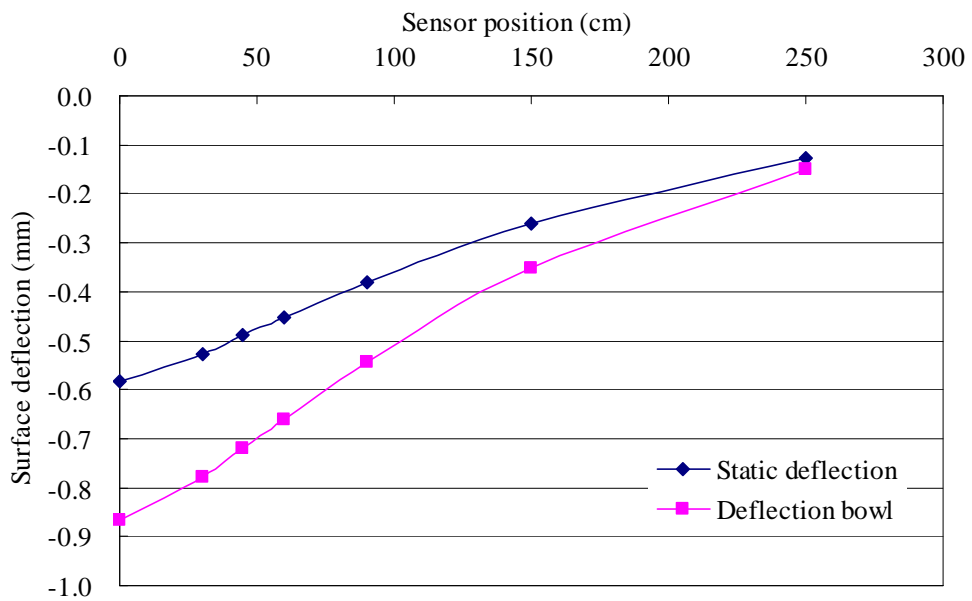


FIGURE 6 Comparison of measured and computed deflections (aircraft load simulator).

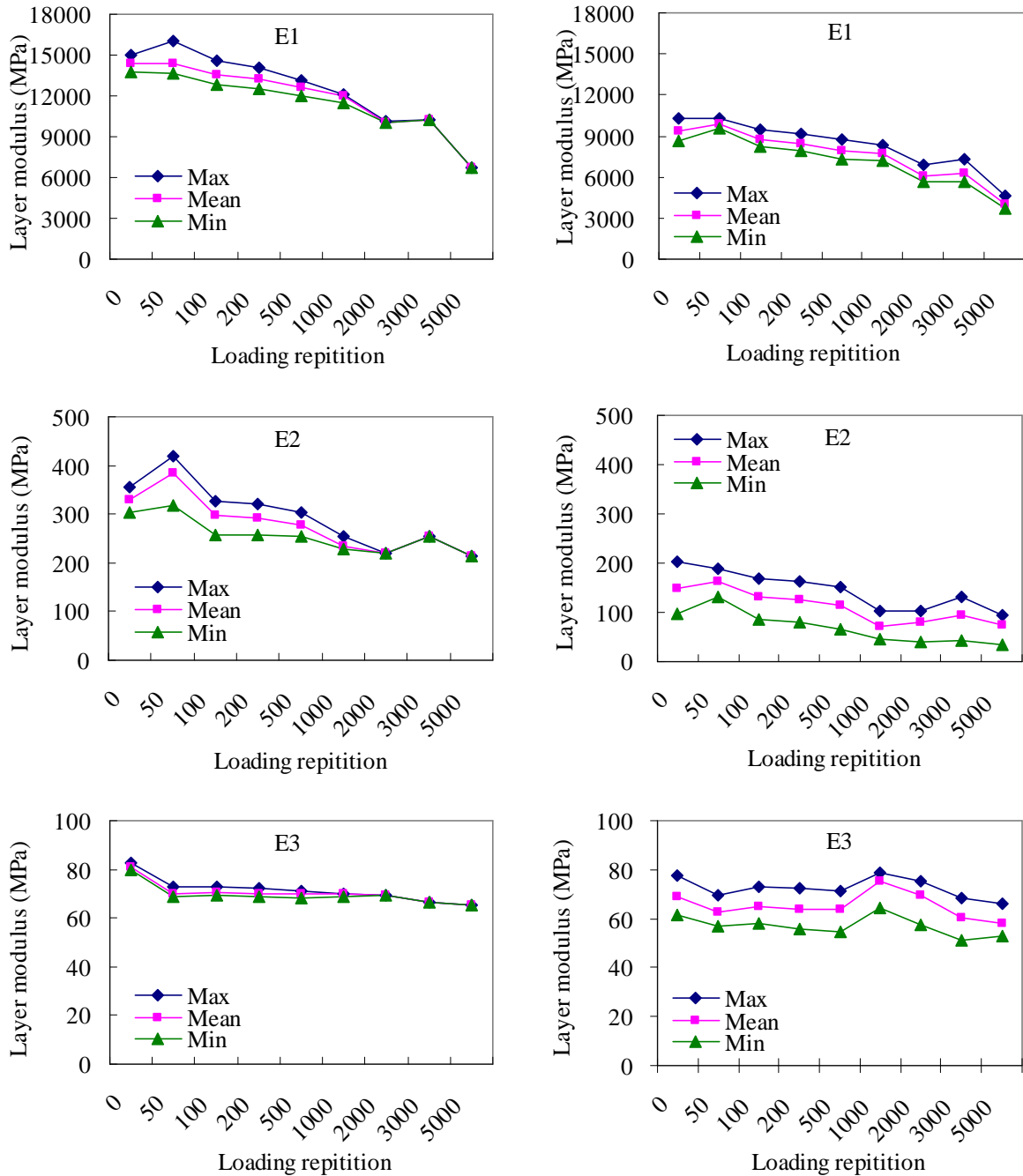


(a) Measured FWD data



(b) Comparison of deflection bowl and static deflection

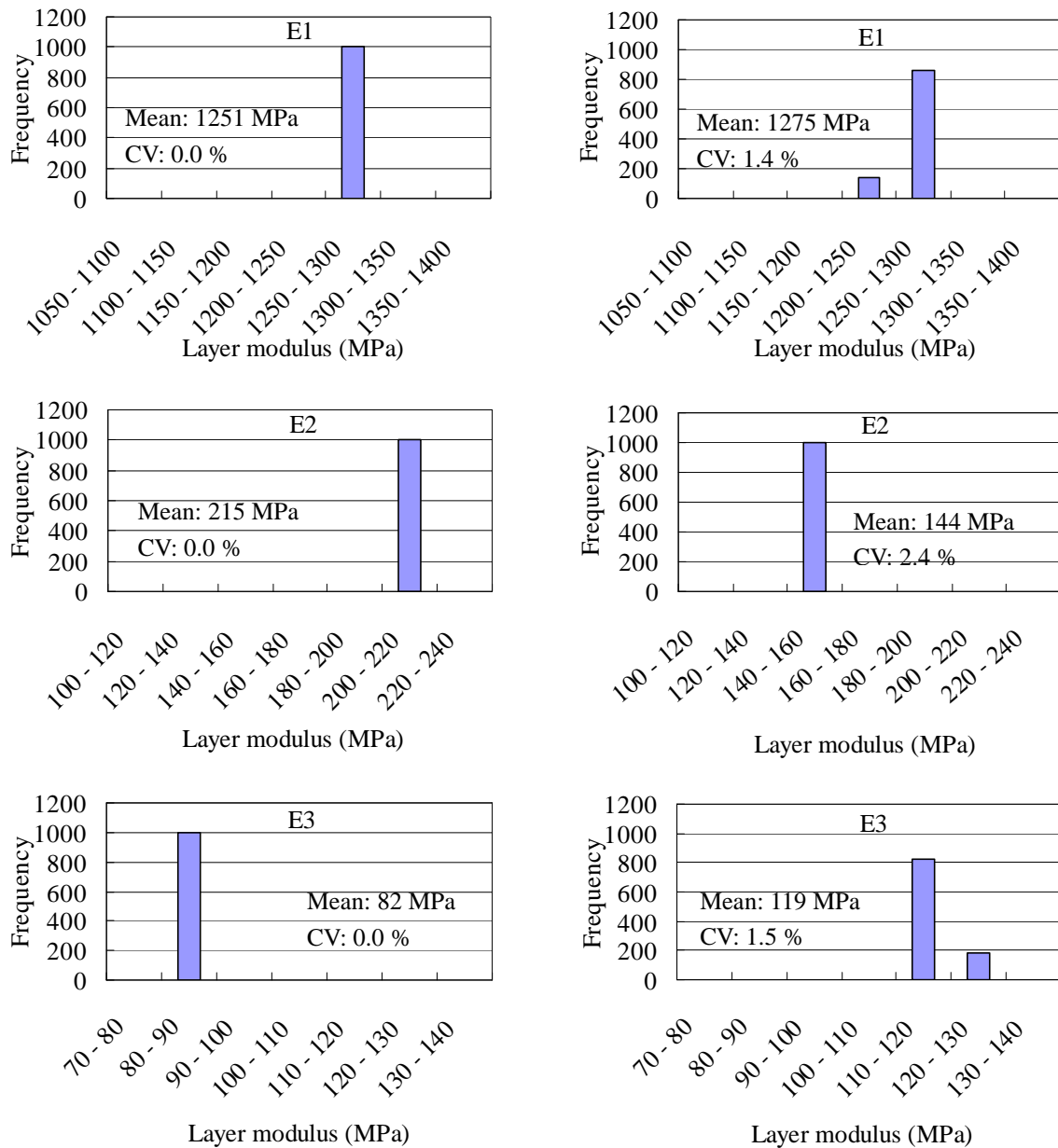
FIGURE 7 Measured FWD data, and comparison of deflection bowl and static deflection (aircraft load simulator).



(a) Static backcalculation

(b) Dynamic backcalculation

FIGURE 8 Maximum, mean and minimum modulus with respect to loading repetitions (aircraft load simulator) □



(a) Static backcalculation

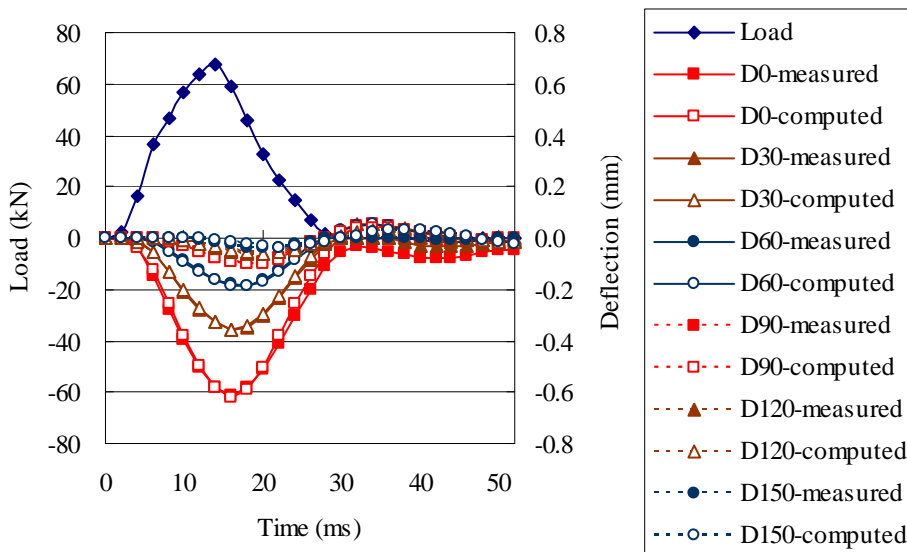
Layer damping coefficients

	C1	C2	C3
Max (kN□s/m)	5.609	0.2864	0.2157
Min (kN□s/m)	4.089	0.0052	0.1608
Mean (kN□s/m)	4.396	0.2287	0.1730
CV (%)	9.3	32.6	8.4

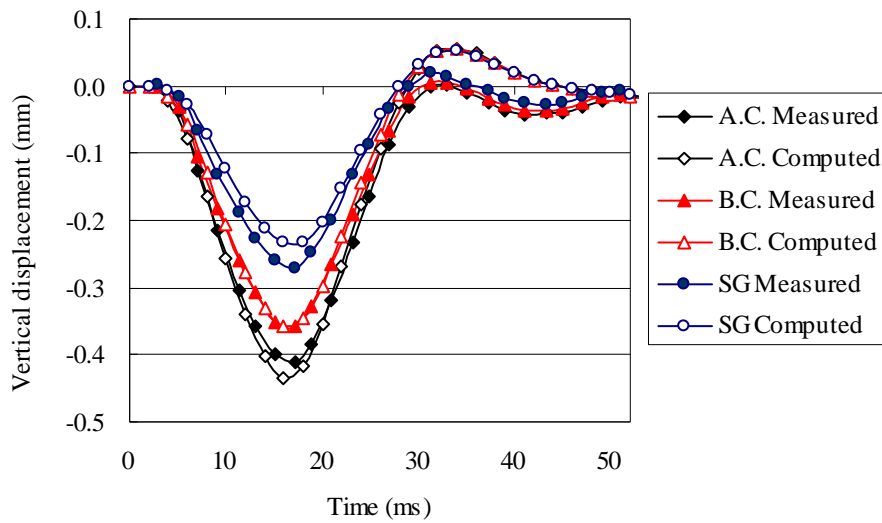
(b) Dynamic backcalculation

FIGURE 9 Frequency distributions of static and dynamic backcalculation results (Texas LTPP data) □

(CV : a coefficient of variation)



(a) Surface deflections



(b) Vertical displacements at MDD sensor locations

FIGURE 10 Surface deflections and vertical displacements at MDD sensor locations (Texas LTPP data)

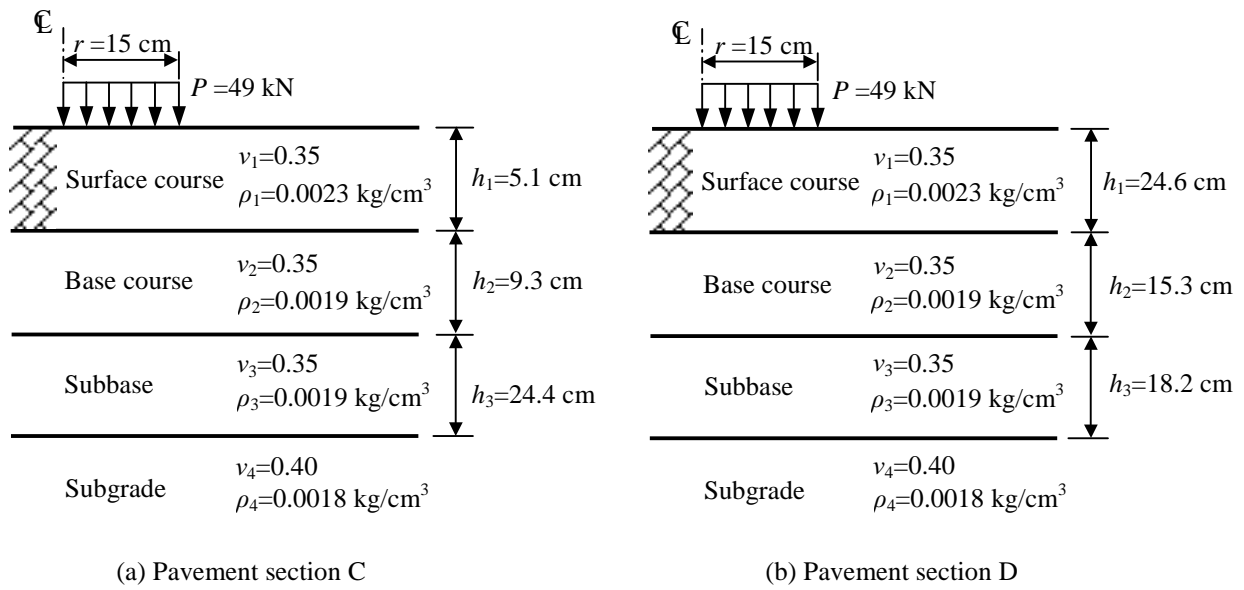


FIGURE 11 Road test sections in Japan.

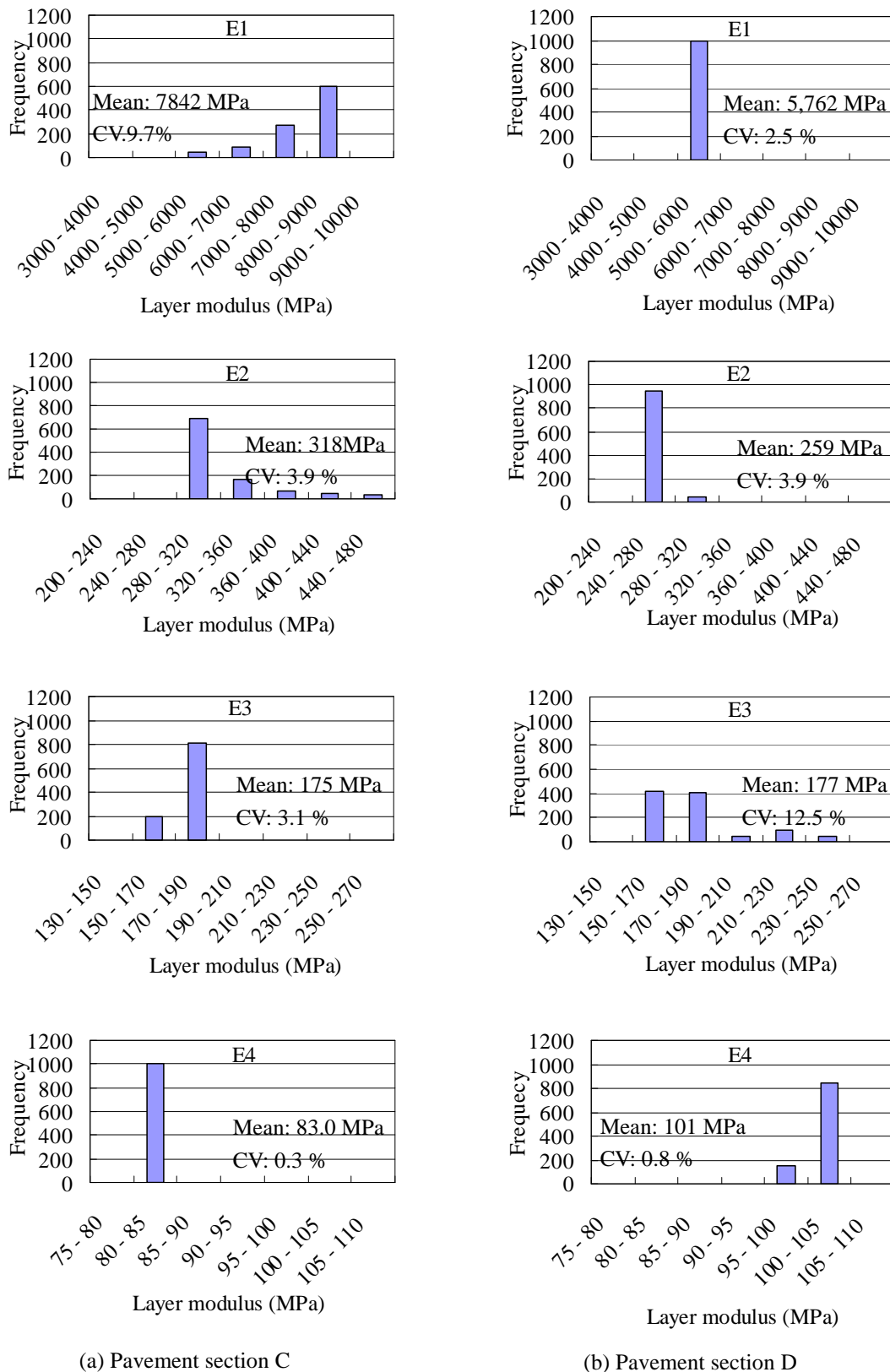
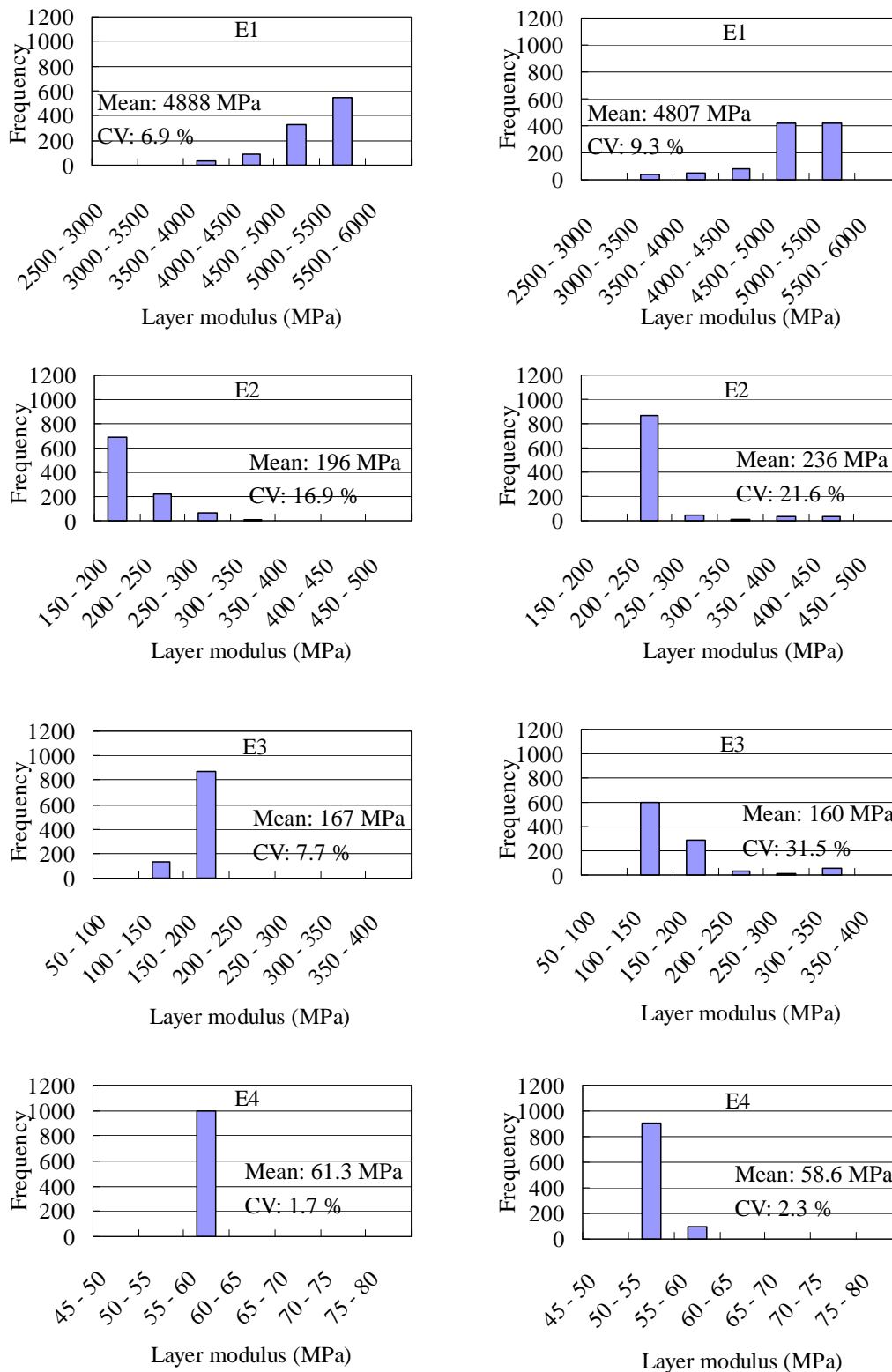


FIGURE 12 Frequency distributions of static backcalculation (test site in Japan).

CV : Coefficient of Variation



(a) Pavement section C

(b) Pavement section D

FIGURE 13 Frequency distributions of dynamic backcalculation (test site in Japan).

(CV : Coefficient of Variation)